FACTA UNIVERSITATIS
Series: **Electronics and Energetics** Vol. 38, Nº 2, June 2025, pp. 305 - 336
https://doi.org/10.2298/FUEE2502305M

Original scientific paper

COMPARATIVE INVESTIGATION OF VISIBLE TO SWIR LASERS FOR TERRESTRIAL FSO LINK ANALYSIS UNDER VARIOUS METEOROLOGICAL CIRCUMSTANCES

Shibabrata Mukherjee[1], Bidrohi Bhattacharjee[2], Pradip Kumar Sadhu[2], Heranmoy Maity[3]

[1]Jadavpur University, Kolkata, West Bengal, India
[2]Department of Electrical Engineering, Indian Institute of Technology (Indian School of Mines), Dhanbad, Jharkhand-826004, India.
[3]Pailan College of Management & Technology, Kolkata, India

ORCID iDs:		
	Shibabrata Mukherjee	https://orcid.org/0000-0002-9561-5504
	Bidrohi Bhattacharjee	https://orcid.org/0000-0001-7622-8034
	Pradip Kumar Sadhu	https://orcid.org/0000-0001-8104-5232
	Heranmoy Maity	https://orcid.org/0000-0002-8305-4818

Abstract. *This paper compares coherent optical sources operating in the visible to short wavelength infrared (SWIR) spectral bands at various wavelengths, such as lasers operating in longer-range terrestrial free space optical links under varying atmospheric circumstances. For the link range of five kilometers, different laser sources have been taken into consideration in this comparison research. For instance, two visible wavelengths (532 nm, 640 nm), two near infrared wavelengths (NIR) (808 nm, 980 nm), and one short wavelength infrared (SWIR) (1550 nm) have all been discussed. Additional characteristics include a 100 MHz data transmission frequency and Return to Zero On-Off Keying (RZ-OOK) modulation technique. Fog, rain, snow, turbulence, and other atmospheric phenomena have a significant impact on the terrestrial FSO link. Thus, in order to retain dependable connection performance and recover the conveniently supplied information in inclement weather, transmitted optical power is a crucial requirement. Other parameters like optical power attenuation, signal to noise ratio (SNR), bit error rate (BER), etc. have been analyzed at the receiver end using proper optics for each wavelength at a distance of 5 km in various adverse atmospheric conditions. From the link analysis computation, it has been revealed that the link margin for 1550 nm, 980 nm, 808 nm, 640 nm, and 532 nm Lasers are about 63.1 dB, 60.6 dB, 59 dB, 57 dB, and 56 dB respectively for 5 km link range at adverse atmospheric scenario.*

Key words: *Adverse atmospheric conditions, Link Margin, Optical power attenuation, Optical Wireless Communication, SWIR; Visibility, Terrestrial FSO link*

Received November 27, 2024; revised December 3, 2024, January 11, 2025, February 1, 2025, and February 11, 2025; accepted February 16, 2025

Corresponding author: Bidrohi Bhattacharjee
Department of Electrical Engineering, Indian Institute of Technology (Indian School of Mines), Dhanbad, Jharkhand-826004, India
E-mail: onlybidrohi@gmail.com

1. INTRODUCTION

In modern times, LASERS are effectively used for a variety of tasks, including welding, surgery, holography, range finding, optical communication, etc. One of the key uses for next-generation communication networks is free space optical communication. The FSO communication system is becoming more and more popular because to its long-range operation, fast data rate, immunity to electromagnetic interference, high level of security, and lack of need for underground fibre cables or spectrum licenses [1]. In a terrestrial free space optical communication system, message signals or information can be transmitted through an unguided channel using different wavelength coherent optical sources between two points. This unguided channel can be established in different mediums like atmosphere, underwater, combination of free space and under water and space (inter-satellite), but in this article terrestrial free space communication link is the main concern. Because the functioning of this sort of system is heavily dependent on the weather, installation of this type of system in any place or region requires a thorough investigation of the local meteorological conditions. For installation of this type of system in any location or area, the proper survey of the weather condition for that particular location or area is required because the performance of this system is very much weather dependent. Since the weather varies depending on the location, the system's ability to work successfully at a given distance depends on the computation of sent and received power. In both favorable and unfavorable weather circumstances, the system's ability to maintain an appropriate signal to noise ratio (SNR), minimal bit error rate (BER), and minimum received power at a given distance is crucial.

In addition, another crucial factor in the terrestrial FSO communication system is connection distance, or data bandwidth. For visible light communication, visible wavelengths between 400 and 700 nm are often utilized. Terrestrial FSO systems employ wavelengths in the near infrared (780nm–1400nm) and shortwave infrared (1400 nm–3000 nm), among other ranges. The predominant spectral wavelength range for this kind of long-distance terrestrial communication system, when it comes to SWIR wavelengths, is 1530 nm–1560 nm [2][3][4]. When compared to 1550 nm laser sources, visible wavelength and near-infrared laser sources are often less expensive [5][6]. As free space optical communication technology has different attractive features, the local area network (LAN), metropolitan area network (MAN), and wide area network (WAN) connections may be established using FSO. As a result, in different countries, many researchers are involved in this field of research and some of their works have been reported in this section. Some of the articles are focused on comparative studies of different wavelength laser sources in different environmental conditions like fog, rain, etc. and attenuation of the sources has been reported. In this regard, three optical wavelengths—850, 950, and 1550 nm—with a link distance of one kilometer and three primary atmospheric conditions—fog, rain, and humidity—have been taken into consideration in [7]. Here, an optical source operating at 1550 nm has reached 10^{-6} BER at a link range of 0.95 km, whereas optical sources operating at 850 nm and 950 nm have achieved the same BER at 0.84 km and 0.86 km, respectively, of same link distance. Two optical wavelengths, 850 nm and 1550 nm, are compared in another article [8] with a varied connection distance ranging from 0.2 km to 1.6 km and corresponding differences in visibility from 0.2 km to 1.2 km. From this article, it has been understood that 850 nm optical source provides the 9.49 dB and 1550 nm optical source provides the 14.87 dB link margin at a link distance of 1.6 km and visibility 1.2 km respectively. In [9], three wavelengths like 850 nm, 1310 nm & 1550 nm, with a link range of 0.5 km and atmospheric attenuation of 70 dB/km were considered. At the receiver end it has been found that those three optical sources gave -40.8880 dBm, -40.9990 dBm, -40.7786 dBm signal power respectively. A 1550 nm laser was employed for experiments in [10], and a 100 Mbps data throughput was taken into consideration when using the RZ encoding approach. The laser's maximum power of 5 mW is taken into consideration, and its diameter is 3 mm. Temperature and wind speed are the two categories of meteorological parameters that have been taken into account for the link reliability study. Different wind speeds have been established, with a maximum speed of 15 km/h being taken into consideration. When it comes to temperature, 500^0 C is thought to be the maximum average temperature. It is evident from the experiment's outcome that when temperature and wind speed increased, the Q factor also dropped. As a result, in both scenarios—the rising temperature and wind speed scenario—BER performance has deteriorated. Another investigation, conducted in [11], using a laser source with a wavelength of 1550 nm and a data speed of 10 Mbps. The OOK modulation approach was taken into consideration. A 0.5 x 0.5 x 5 m3 rain chamber has been introduced in this experiment. For this experiment, a maximum rain rate of 210 mm/hr was taken into consideration. Based on the least square mean equation method, the estimated values of α and k are 0.91 and 0.63, respectively. The discovery aids in power margin reporting and enhances system performance while implementing an optical link in regions with heavier precipitation. The optical power attenuation increased along with the rain rate, which led to deteriorate in the BER value. Another investigation with an 850 nm wavelength laser source and 10 Mbps data transmission was conducted in [12]. Two sorts of elements have been introduced in this experiment: Single Input Multiple Output (SIMO) and aperture averaging. The two previously mentioned methods were implemented in order to enhance the system. In deteriorating atmospheric (rainy) circumstances, the SIMO technique outperformed the aperture averaging technique. A hybrid FSO-RF system has been introduced in [13]. This system has been exposed to three different kinds of meteorological anomalies: fog, rain, and snow. Maximum fog visibility was 1.5 km, maximum rain rate was 250 mm/hr, and maximum snowfall rate was 10 mm/hr. According to the testing results, data was communicated over the FSO link with an effective FSO transmission range of up to 1 km during the wet season and up to half a km during fog and snow events for a favourable BER value. Another investigation with an 850 nm wavelength laser source and 10 Mbps data transmission was conducted in [14]. Direct intensity modulation (D-IM), pulse width modulation (PWM), subcarrier intensity modulated frequency shift keying (SIM-FSK), subcarrier intensity modulated amplitude modulation (SIM-AM), subcarrier intensity modulated phase modulation (SIM-PM), and subcarrier intensity modulated frequency modulation (SIM-FM) are some of the modulation schemes that have been introduced in this study. PWM and SIM-FSK perform better in more precipitation.

A Ro-VLC system with a 25 Mbps data throughput was introduced in [15]. Three wavelengths of LEDs—650 nm, 530 nm, and 450 nm—have been employed in this investigation for communication. For this work, two encoding methods—RZ and NRZ—have been taken into consideration. When compared to the RZ encoding approach, the RZ encoding technique yields better BER values. A 40 Gbps FSO communication system that is affordable has been demonstrated in [16]. The study has taken into account wavelengths between 1550 and 1553 nm, with a link distance ranging from 100 to 2000 m. This communication system introduced the EDFA amplifier. In various visibility circumstances (from bad to clear), the link dependability has been improved with the use of this amplifier. A 10 x 100 Gbps MDM-WDM terrestrial FSO communication system was proposed in [17]. The system incorporates a dual polarization-quadrature phase shift keying (DP-QPSK) modulation technology. The wavelengths ranged from 1550 nm to

1554 nm, and the link distance was evaluated between 1.2 and 20 km. 850 nm and 851 nm wavelength lasers have been taken into consideration in a low-cost, high-speed Ro-FSO communication system that was proposed in [18]. To transmit four 10 GHz channels, WDM and MDM techniques are combined. In clear weather conditions, all channels have successfully communicated data at a link range of 1200 m. In low, medium, and intense fog situations, on the other hand, data may be transferred with a link range of 570 m, 500 m, and 440 m, respectively, while maintaining a Bit Error Rate of 10^{-3}. A mode division multiplexing (FSO) system with a 20 Mbps data transmission speed was introduced in [19] for healthcare infrastructure. In a clear weather situation, the data was successfully delivered over a 27 kilometer link distance. The identical system has been examined under low, medium, and strong fog (visibility) circumstances. Under strong foggy, condition, the performance has deteriorated.

In [20], an 850 nm wavelength has been used to depict a hybrid division multiplexing (MDM) and polarization division multiplexing (PDM) based Ro-FSO system. Various meteorological conditions have been used to test the aforementioned link. According to the simulation's outcome, 3400 meters might be reached as the link distance in a clear weather scenario, with a BER of 10^{-3} that is acceptable. However, due to attenuation, the suggested MDM-PDM-Ro-FSO link could only tolerate up to 1000 m when the weather changed to partial haze/rain. Furthermore, the suggested link could only endure up to 650 meters with an acceptable bit-rate error (BER) when the meteorological state changed from partial haze/rain to dense fog/heavy rain.

This section includes certain particular geographic regions and meteorological data collected during testing to improve the findings' dependability. A FSO-based experimental investigation using an 808 nm laser source was carried out in Changchun, Jilin, China in [21]. This experiment has taken into consideration the OOK modulation approach at speeds of 100 Mbps and 500 Mbps across a 6.2 kilometre link distance. It has been assessed how much of an impact scintillation has on the FSO link for a whole day. This study found that for both of the studied data rates, the BER values increased when the scintillation index increased over 0.2. Similarly, another FSO-based work that was presented in Saudi Arabia may be found in [22]. This experiment has examined the FSO system's optical power attenuation in a dusty situation. A $90 \times 40 \times 40$ cm^3 artificial dust box and a Laser source with a wavelength of 1520 nm were taken into consideration for this experiment. This study indicates that dust attenuation of light is approximately seven times that of fog attenuation. In Qatar, another FSO experimental study has been conducted [23]. This experimental effort has taken into consideration a 1550 nm laser source operating at 1 Gbps data speed over a 600 m connection distance. In this experiment, the performance of the packet delivery ratio (PDR) has been measured in several seasons, such as winter, summer, spring, etc., with varying levels of scintillation throughout the day. This study indicates that PDR performance is higher in the winter than in the summer. With the aid of theoretical and simulation models, feasibility studies for free space optical (FSO) communication for the city of Bhubaneswar are described in [24]. The last five years' worth of visibility, precipitation, and wind speed data for Bhubaneswar are used to compute the atmospheric losses. The outcome indicates that the highest FSO distance that can be achieved for Bhubaneswar in poor visibility conditions is 633.5 meters when the loss is 28 dB. In clear weather, however, an FSO connection distance of 1558 meters was obtained with a loss of 16.7 dB. In [25], a software simulation-based work has been carried out in Lahore, Pakistan. From this study, it has been shown that the lowest visibility of dust was 2.6187 km & the highest visibility was 5.2936 km in that place, as a result, the attenuation was 8.1236 dB & 4.8256 dB respectively. The maximum rain rate of 150 mm/hr and the related attenuation of 30 dB/km were taken into consideration. The highest allowed transmitted laser power is 20 dBm, and for link distances up to 2 km, the allowable attenuations for dust and rain rate are 8.1 dB/km and 11.59 dB/km, respectively. In [26], an experiment in Milan, Italy, revealed that the greatest attenuation caused by snowfall was 21 dB, and that it occasionally exceeded 45 dB/km, leading to connection failure. A work based on simulation has been done in [27]. The wintertime fog in Delhi, India has been taken into consideration in this study. This research examines five years' worth of data, and from that data, it can be found that January has the lowest visibility, with visibility of about 0.9 km and a corresponding attenuation of 3.64 dB/km. The 850 nm wavelength has been taken into consideration in this study. It is suggested that transmitting power between 25 and 35 dBm be employed for the best transmission range of 6 to 8 Km in order to provide error-free data transmission during the fog months. A fog attenuation model has been developed from the observed values of the optical attenuation of fog in several locations of Europe and the United States, as published by the authors in [28]. According to this study, in moderate fog, 12 dBm of transmitted optical power is required to achieve BER (10^{-3}) under 500 m connection length.

Some commercially available, visible to SWIR laser sources with wavelengths of 532 nm, 640 nm, 808 nm, 980 nm, and 1550 nm have been analyzed in this current article. Each wavelength (532 nm, 640 nm, 808 nm, 980 nm, 1550 nm) of Laser source is transmitted with 30 dBm peak optical power, at a link range of 5 km, data transmission frequency of 100 MHz, considering Bit Error Rate (BER) 10^{-6} with relevant 16 dB Signal to Noise ratio along with suitable optics corresponding to their relevant technical specifications. Here main atmospheric condition has been considered as fog. An optical modulator unit, which modulates the continuous wave laser beam in accordance with the incoming message signal, has been taken into consideration for the establishment of the terrestrial FSO link. The analytical findings section discusses several computations related to link margin with the considered wavelengths in different visibility circumstances. Several visibility (for low to high visibility) and their attenuation (dB) at five-kilometer distances are assessed in this article. This article also covers the use of carefully selected optics to reduce beam divergence loss.

2. Establishment of Terrestrial FSO Link

The terrestrial FSO system comprises mainly three units- transmitter, receiver, and free space terrestrial channel. For reliable and rugged communication system, different optical accessories like lens, optical filter, beam expander, etc. are required in clear as well as adverse weather conditions.

The transmitter unit consists of continuous wavelength Laser source, optical modulator unit and beam expander. The beam expander is a combination of concave and convex lenses. The beam expander is used at the transmitter side to reduce the beam divergence with the same power expansion; as a result, beam diameter at receiving end as well as beam divergence loss is decreased at the longer distance [29][30]. The specifications of the Lasers and the beam expander are given in Table 1.

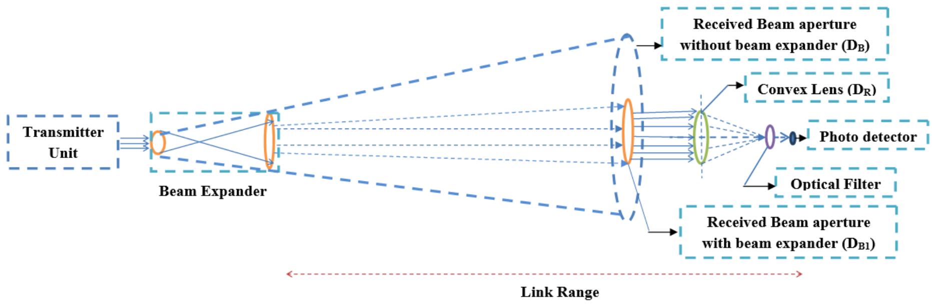

Fig. 1 Effect of different optics used in terrestrial FSO system [30][31]

The beam diameter (D_B) at the receiver side is defined by equation (1) [32]

$$D_B = D_L + (L * \tan\theta) \tag{1}$$

ϴ represents Laser beam divergence angle, L indicates Terrestrial FSO link distance, D_L defines Laser beam aperture, as ϴ is very small, tan ϴ can be written as ϴ. After using the beam expander at the transmitter side, the beam diameter at the receiver side can be obtained from equation (2). The effect of the beam expander and other optics is illustrated in Fig 1.

$$D_{B_1} = (MF * D_L) + (L * \tan(\frac{\theta}{MF})) \tag{2}$$

D_{B1} indicates Beam diameter at the receiver side using beam expander, MF represents Magnifying factor of beam expander

The atmospheric channel consists of different gas, molecules, aerosols, etc., with different hazards like fog, rain, dust, snow, etc. The attenuation of laser power of different hazardous atmospheric conditions is discussed in the next section.

Table 1 Specifications of Laser sources, beam expander

Sl No.	Parameter	Value
1.	Laser wavelength	532nm, 640nm, 808nm, 980nm, 1550nm
2.	Beam Divergence Angle	0.1 mrad
3.	Transmitted peak Laser power	1 Watt
4.	Beam Waist	2.5 mm
5.	Operating Mode	Continuous-wave (CW), Tunable optical power
5.	Transmittance of beam expander	96 %
6.	Magnifying Power of beam expander	20x
7.	Entrance aperture of beam expander	2.5 mm
8.	Exit aperture of beam expander	50 mm

After traversing the aforesaid free space terrestrial channel, the modulated transmitted optical signal must be received by the properly aligned photodetector. Different optical accessories like lens, optical filter, etc. are incorporated or attached before the photo-detector for reliable and rugged communication [33]. To accumulate or converge the transmitted beam at a particular focal length at the receiver side, convex lens is mainly used. An optical filter rejects the unwanted radiation and passes the desired wavelength beam. In this comparative study, two types of photodetectors are considered. For 532 nm, 640 nm, 808 nm Laser sources, Silicon-based, PIN photodetector is considered which is denoted as photodetector 1 and for 980 nm and 1550 nm Laser, InGaAs [34] based PIN detector is considered which is denoted as photodetector 2. The specifications of photo-detector 1 and 2, are given in Table 2.

Table 2 Specifications of Photo-detector 1 and 2

Sl. No.	Parameter	Photo-detector 1	Photo-Detector 2
1.	Operative Wavelength Range	320 nm – 1000 nm	850 nm – 1700 nm
2.	Active Diameter	0.4 mm^2	0.3 mm^2
3.	Responsivity at peak (R_λ)	0.51 A/W, 800 nm	1 A/W, 1550 nm
4.	Responsivity	($R_{\lambda 1}$) at 532 nm- 0.35 A/W ($R_{\lambda 2}$) at 640 nm- 0.415 A/W ($R_{\lambda 3}$) at 808 nm- 0.505 A/W	($R'_{\lambda 1}$) at 980 nm- 0.64 A/W ($R'_{\lambda 2}$) at 1550 nm- 1 A/W [35][36]
5.	3 dB Bandwidth	125 MHz	125 MHz
6.	Dark Current (i_d)	5 nA	2 nA

The materials that are used for the fabrication of photodetectors or photodiodes greatly influence the characteristics of the detectors or diodes itself. Amongst them, one of the mentionable characteristics is their response to particular wavelengths. The sole reason behind this varying response to particular wavelengths is that the different materials, used in the manufacture of the concerned photodetectors or photodiodes, generate photons, which in turn is responsible for the generation of sufficient energy for the electrons to travel across the bandgap inducing current across the detectors or diodes. The wavelength sensitivity of Silicon is 190 nm to 1100 nm and Indium Gallium Arsenide is sensitive for 850 nm - 1700 nm wavelength. Besides the wavelength sensitivity of the material of the photodetector, another key factor is the level of noise is produced in the photodetector which can have a major impact on the performance of the system [37].

Quantum efficiency is another important parameter of the photodetector, which is defined as the photodetector capability to convert light energy to electrical energy and it is expressed in percentage which is expressed in equation (3) [38]. Quantum efficiency (η) is related to the responsivity (A/W) of photodetector or photodiode, photon energy of incident light.

$$\eta = \frac{R_\lambda * E}{q} \tag{3}$$

R_λ denotes Responsivity of photodetector, E indicates Energy of incident photon on photodetector, q represents Charge of electron.

The energy of a particular wavelength of the photon is given by equation (4) [38]

$$E = \frac{h * C}{\lambda} \tag{4}$$

The quantum energy for the above-mentioned wavelength is given in Table 3.

Table 3 Quantum efficiency of photodetector, quantum energy of different wavelength laser

Sl. No.	Different Wavelength of Lasers (nm)	Quantum energy of Wavelength (J)	Responsivity of photodetector of different wavelength Lasers(A/W)	Quantum Efficiency (%)
1.	532	3.7×10^{-19}	0.35	~ 81
2.	640	3.12×10^{-19}	0.415	~ 81
3.	808	2.56×10^{-19}	0.505	~ 81
4.	980	2.03×10^{-19}	0.64	~ 81
5.	1550	1.3×10^{-19}	1.00	~ 81

The specifications of convex lens & optical filter are given in Table 4. These are applicable for above mentioned all the wavelengths of coherent beam optical sources. Above mentioned units and accessories are shown in Fig 1.

Table 4 Specifications of Convex lens & optical filter

Sl. No.	Parameter	Value
1.	Diameter & Focal length of lens	75 mm, 300 mm
2.	Transmittance of lens	98%
4.	Diameter of optical filter	25 mm
5.	FWHM of optical filter	10 nm
6.	Transmittance of optical filter	50%-70%

The block diagram of the terrestrial FSO system is shown in Fig 2. In this system, continuous wave coherent optical beam has been modulated by an optical modulator unit according to the coming message signal. The optical modulator is used to shutter the coherent beam on and off.

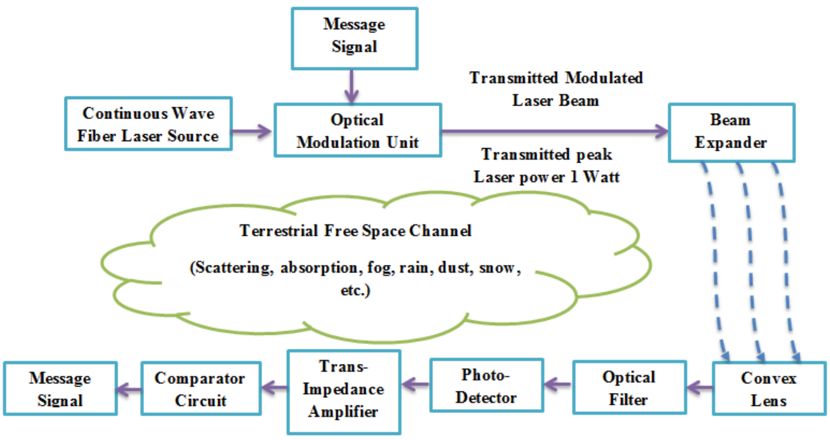

Fig. 2 Block diagram of terrestrial FSO system [38]

By applying the digital data input which is coming from the message signal fed to the optical modulator unit, the optical modulator modulates the laser beam according to the message signal. The modulated coherent beam is fed to the transmitting optics i.e., the beam expander. The transmitted modulated beam is propagated through terrestrial free space, and then it is fallen on the convex lens. The size of the convex lens is an important factor to reduce the background noise of the receiver side, the size of the convex lens may be equal to the beam size of the receiver side. Larger size of the convex lens may create background noise in the FSO system and the small size (less than the beam size of the receiver side) of the convex lens may create the beam expansion loss. After collecting the modulated coherent beam from convex lens, it is fed to optical filter. Then desired wavelength, noise-free, the modulated beam reaches to the properly aligned photo-detector. By trans-impedance amplifier, the current signal in photo-detector has been converted to amplified voltage level. The main advantage of using the trans-impedance amplifier is that it has a high dynamic range, the numbing effect of negative feedback makes the stability of receiver response over time, temperature, etc., commendable. A high-speed comparator (around 200 MHz bandwidth) is used for evens out the signal peaks; as a result, a clean signal is obtained.

3. TERRESTRIAL FSO CHANNEL

When the optical coherent source i.e. Laser is propagated through the terrestrial or atmospheric path, scattering and absorption has occurred on the link because gases, particles, aerosols, etc. are suspended in the atmosphere or terrestrial path. The terrestrial FSO link can be attenuated by the different atmospheric precipitations like rain, fog, snow, etc. The precipitations present in the atmosphere vary with season, longitude, latitude of the area. Obviously, near the earth's surface (troposphere), the concentration of particles is high. This type of concentration is low with increasing altitude is also high (in the ionosphere). For a particular terrestrial link range (*L*), the Laser power attenuation through the atmosphere is determined by equation (5) which is called Beers-Lambert law [39]:

$$\tau(\lambda, L) = \frac{P_R}{P_T} = e^{-\gamma_T(\lambda)*L} \tag{5}$$

$\tau(\lambda,L)$ & $\Upsilon_T(\lambda)$ indicates total attenuation or extinction coefficient, P_R indicates received optical power, P_T indicates transmitted optical power.

The attenuation coefficient of aerosols and molecular constituents of the atmosphere is shown in equation (6) [40].

$$\gamma_T(\lambda) = \alpha_m(\lambda) + \alpha_a(\lambda) + \mu_a(\lambda) + \mu_m(\lambda) \tag{6}$$

$\alpha_m(\lambda)$, $\alpha_a(\lambda)$ indicates the molecular and aerosol absorption coefficients, while $\mu_a(\lambda)$, $\mu_m(\lambda)$ indicates the molecular and aerosol scattering coefficients respectively.

Generally, atmospheric absorption is wavelength dependent phenomenon, molecular absorption of different wavelengths is different. Generally, the total molecular and aerosol absorption coefficient is very less than the molecular and aerosol scattering coefficient. So, Equation (6) can be written as which is represented in equation (7)

$$\gamma_T(\lambda) = \mu_a(\lambda) + \mu_m(\lambda) \tag{7}$$

The scattering effects are very much wavelength (λ) dependent, as well as scattering effect depends upon the radius (*R*) or size of the molecule, aerosols (fog, mist, etc.).

According to size parameter ($n_o = 2\pi R/\lambda$), mainly three types of scattering phenomenon can be observed which is depicted in Fig. 3[41][42].

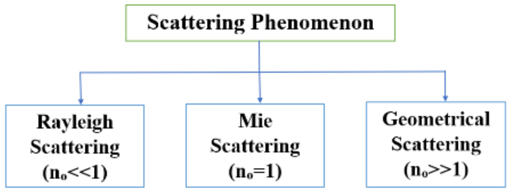

Fig. 3 Classification of scattering phenomenon

In this article, the effect of fog is only considered, hence the effect of fog on FSO channel has been discussed below:

3.1. Effect of Fog

The term 'fog' is very small, but the impact on the terrestrial FSO link is high. The radius of the fog droplets in between 1~20 µm, the scattering phenomenon occurred mainly Mie or sometimes geometrical scattering in foggy conditions. Fog contributes the major optical power attenuation because the terrestrial-based FSO system wavelength band (0.5µm - 2µm) falls within the fog particle droplet size. The attenuation coefficient (dB/km) can be measured with a common Mie scattering empirical model which is related to very much visibility, the wavelength of the optical source is given in equation (8)[43][44].

$$A_F(\lambda) = \left(\frac{3.91}{V}\right) * \left(\frac{550}{\lambda}\right)^q \tag{8}$$

$A_F(\lambda)$ represents Attenuation coefficient, V indicates Visibility (km), λ depicts Wavelength (nm) of optical coherent source, q indicates Constant parameter which is related to particle size distribution and visibility.

Total attenuation (L_{Fog}) (dB) due to fog for a particular link range is given by equation (9)[45][46],

$$L_{fog} = -10 * \log(e^{-A_F(\lambda)*L}) \tag{9}$$

The visibility range of dense fog to thin fog varies between 150 m to 2000 m. According to the visibility range, the attenuation coefficients are also varying for a particular optical wavelength source. The value of q is defined by two models which are given in Table 5. The attenuation (dB) due to fog with different visibility (km) and wavelength of Laser at link range of 5 km is illustrated in Fig 4.

Table 5 The value of q according to different visibility range [47][48]

Sl. No.	Visibility Range (m)	Value of q (According to Kim Model)
1.	V>50000	1.6
2.	6000<V<50000	1.3
3.	1000<V<6000	0.16V+0.34
4.	500<V<1000	V-0.5
5.	V<500	0

The attenuation is determined using above mentioned formula and for *q* value, Kim model is used. From the figure, it has been shown that the attenuation (dB) for visibility, SWIR Wavelengths Laser source is less attenuated compared to other Wavelengths.

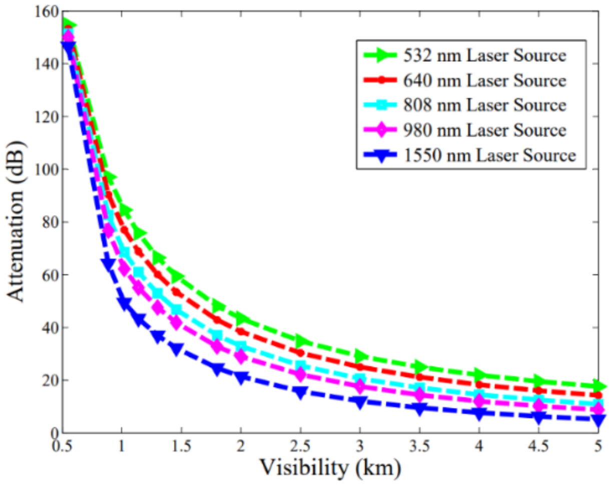

Fig. 4 Lasers power attenuation due to fog vs Visibility

The KIM model was utilized for this simulation, and the value of q was utilized up to 5 km vision range. Equation 9 was utilized to produce Figure 4. Thus, for each visibility range, the value of q was 0, V-0.5, and 0.16V+0.34, as the visibility was considered 500 m – 5 km.

3.2. Effect of Rain

Rain is another important attenuation factor for terrestrial-based FSO system. The rain droplet size (radius) may vary from 100 µm - 10000 µm. As a result, geometrical scattering occurs for rain in the above-mentioned system. In tropical areas or country, where rain has occurred abundantly, there is a big problem with the FSO system. The attenuation coefficient (dB/km) due to rain is in terrestrial-based FSO system can be measured from equation (10) [45]

$$A_R = b * R^a \tag{10}$$

A_R indicates attenuation coefficient, *a* (=0.67) & *b* (=1.076) are parameters that depend upon rain droplet size, rain temperature, etc., and the value is obtained from Carbonneau's model, *R* depicts Rain rate (mm/hr).

The total attenuation (L_{Rain}) (dB) due to rain for a particular link range can be determined by equation (11)[45],

$$L_{Rain} = A_R * L \tag{11}$$

As the attenuation due to rain is mainly occurred for geometrical scattering, so the attenuation is wavelength-independent which is depicted in Fig 5, that is attenuation due to rain (dB) with different rain rates (mm/hr) at a link range of 5 km.

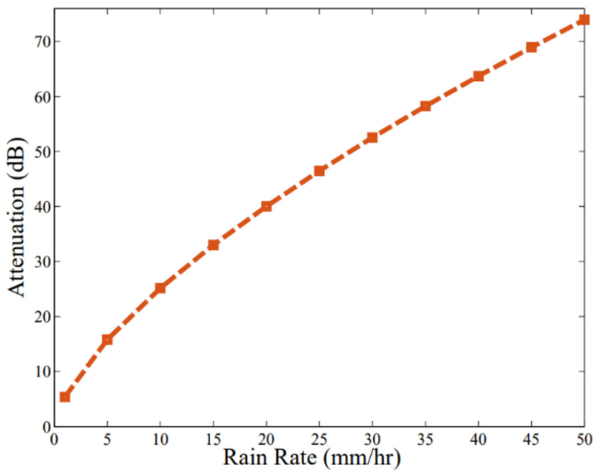

Fig. 5 Lasers power attenuation due to rain Vs Rain rate

The abovementioned equations (10 & 11) have been related to the optical power attenuation due to rain. These equations are directly related to rain rates. But this equation can be represented in terms of visibility. The optical power attenuation due to rain for a certain visibility can be expressed in the equation 12.

$$\gamma_{Rain} = \frac{2.8}{V} \tag{12}$$

3.3. Effect of Scintillation

Radiation from the sun is heating the earth's surface, as a result near the earth's surface air is heated up, becomes lighter, and goes upward. Then the surrounding cool air rushes to that place creating turbulence. This temperature inhomogeneity of the atmosphere creates changes in the refractive index of the atmosphere; this is called scintillation. The more heated air pockets are mixed with other air pocket and as a result, this acts as lens, focusing and defocusing the coherent optical beam as it propagates through the terrestrial path. The size of the air pockets or cells varies from 0.1 cm to 10 m. Attenuation due to scintillation (α_{Scin}) (dB) can be determined from the given equation (13) [37].

$$\alpha_{Scin} = 2\sqrt{23.17*(\frac{2\pi}{\lambda}*10^9)^{\frac{7}{6}}*c_n^2*L^{\frac{11}{6}}} \tag{13}$$

C_n^2 indicates refractive index parameter structure (m$^{-2/3}$), λ indicates Wavelength of the coherent optical source (nm), L = Terrestrial FSO link range (m).

The value of the refractive index parameter structure is different for different turbulence strengths which are given in Table 6. Various models, such as the gamma-gamma distribution model, the lognormal model, the negative exponential model, the k-distribution model, etc., have been utilized for the FSO system analytical purposes in various turbulence intensities. For extremely strong and strong turbulence strength, respectively, the negative exponential model and the k-distribution model are employed; for lower turbulence strength, the lognormal model is employed; and for low to strong turbulence strength, the gamma-gamma distribution is employed [49][50][51]. Since high to low turbulence strength has been taken into consideration in the current article, the gamma-gamma distribution model has been taken into consideration for this simulation.

Table 6 Value of refractive index parameter structure for different turbulence strength

Sl. No.	Low Turbulence	Moderate Turbulence	High Turbulence
1.	10^{-16}	10^{-14}	10^{-13}

Attenuation (dB) due to different turbulent conditions are depicted in Fig 6, 1550 nm Laser source is less attenuated compared to other wavelengths for considering all three types of refractive index parameter structure.

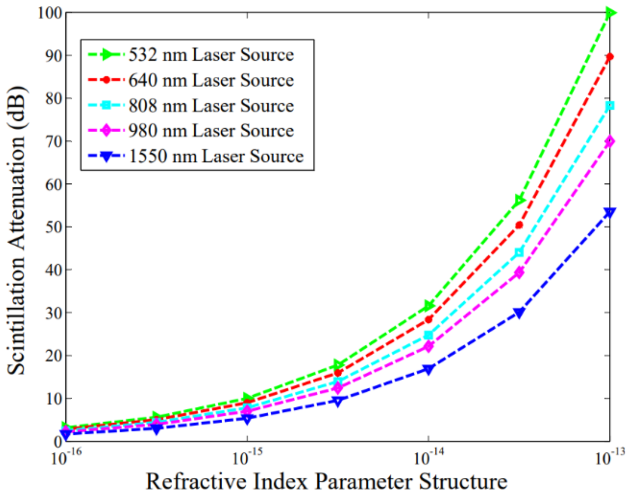

Fig. 6 Lasers power attenuation due to Scintillation Vs Refractive Index Parameter Structure

3.4. Effect of Snow

Mainly two types of snow are observed dry snow and wet snow which can attenuate the terrestrial-based FSO system.

The attenuation coefficient (dB/km) due to snow is in terrestrial-based FSO system can be measured from equation (14). Table 7 represents the different types of snow corresponding to different values of *c* & *d*.

$$A_S = cS^d \tag{14}$$

A_S represents attenuation coefficient doe to snow, S indicates Snowfall rate (mm/hr), *c* & *d* indicates Attenuation constant.

Table 7 Different type of snow corresponding different value of c & d

Sl. No.	Type of snow	Value of *c*	Value of *d*
1.	Wet Snow	$1.02*10^{-5}\lambda + 3.79$	0.72
2.	Dry Snow	$5.42*10^{-5}\lambda + 5.5$	1.38

The total attenuation due to snow (L_{Snow}) (dB) for both dry and wet types of snow for a particular link range can be determined by the multiplication of the attenuation coefficient due to snow and link range which is given in equation (15).

$$L_{Snow} = A_S * L \tag{15}$$

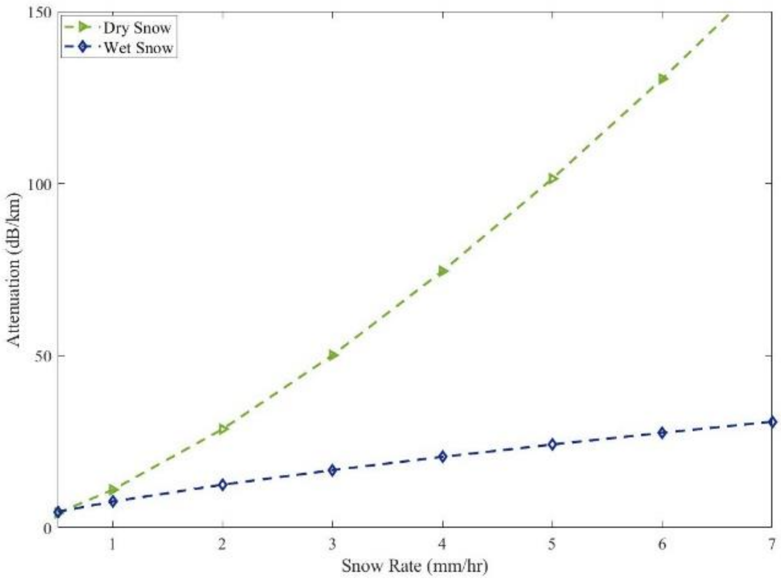

Fig. 7 Lasers power attenuation due to different snow rates

From the Fig 7, it has shown that Laser power attenuation due to dry snow is higher compared to wet snow.

The equation 14 has been represented the optical power attenuation due to snow, this equation is entirely dependent upon the snow rate. Again, the optical power attenuation due to snow has been represented in terms of visibility which is represented by the equation 16.

$$\gamma_{Snow} = \frac{58}{V} \tag{16}$$

Fig. 8 shows the attenuation (dB) for different atmospheric conditions like fog, rain and snow for 5 km link distance. From this figure, it has been clear that attenuation due to snow is highest and the attenuation due to rain is lower compared to fog and snow.

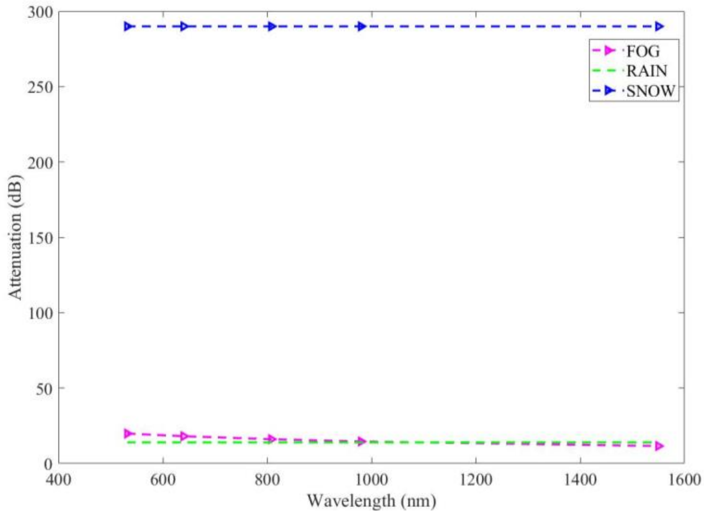

Fig. 8 Attenuation (dB) for different atmospheric conditions like fog, rain, snow for 5 km link distance

4. ANALYTICAL RESULT

In this section, the analytical result of the above-mentioned wavelengths of the coherent optical beam with different parameters like beam divergence loss, power attenuation, BER, SNR, link margin at different wavelengths, etc. in different atmospheric conditions is discussed.

The MATLAB 2019 software version was used to run the whole simulation. Equations (1-29) that have already been covered in the article were used for the MATLAB programming, and the necessary values for these equations' evaluation were taken from Tables 1, 2, and 4, respectively.

4.1. Received Optical Power in Different Visibility

The received optical power, terrestrial-based FSO system can be obtained from the equation (17)[52][53].

$$P_R = P_T * (\frac{D_R^2}{D_{R_1}^2}) * \tau_{atm} * \tau_p * \tau_r * l_{pT} * l_{pR} \tag{17}$$

P_R indicates received optical power, P_T represents Transmitted optical power, τ_{atm} depicts Total atmospheric attenuation for a particular link range, τ_p indicates transmittance of transmitted optics (Transmittance of beam expander) τ_r depicts transmittance of receiver optics (Transmittance of convex lens * transmittance of optical filter), D_R depicts Diameter of receiver lens, D_{B1} represents beam Diameter of Laser Source at the receiver side using the beam expander, l_{pT} indicates pointing loss at transmitter side, l_{pR} represents pointing loss at receiver side

The received power at the 5 km link range, with different wavelengths and different visibility (up to 1.5 km) is depicted in Fig 8. It has been shown from the figure that the received power for the 1550 nm Laser source is more compare to other wavelengths at a distance of 5 km. and different visibility ranges. The ratio of the receiver aperture (D_R) (convex lens aperture) to laser beam diameter (using beam expander) at the receiver side (D_{B1}) is maintained to 1 for eliminating the beam expansion loss.

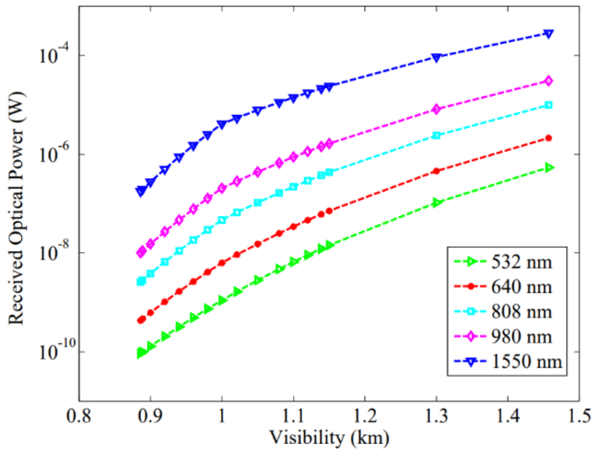

Fig. 9 Received optical power Vs Visibility

Since rain causes optical power attenuation, which is a phenomenon that is independent of wavelength, the power attenuation caused by those anomalies is the same for all wavelengths that are taken into consideration at a link range of five kilometers. Equation 17 has been used to imitate Fig. 9, and it has also been used to simulate Fig. 10, 11, and 12. When the weather is taken into account, the atmosphere transmittance has altered. Equation 8 is applied when the foggy weather condition is taken into account. Likewise, equation 10 is applied when rainy circumstances are taken into account. Likewise, equation 14 is employed to assess the attenuation of various snow kinds.

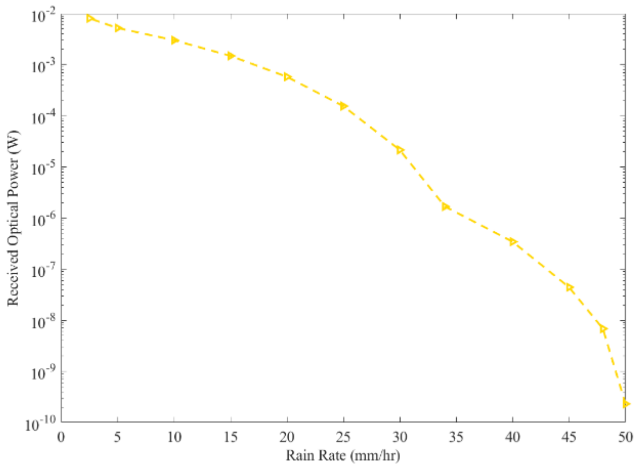

Fig. 10 Received optical power Vs different rain rates

Fig. 10 refers the received optical power for different rain rates conditions.

Since varying snow conditions cause optical power attenuation, which is a phenomenon regardless of wavelength, the power attenuation caused by those anomalies is the same for all wavelengths taken into consideration for a 5 km connection range.

The optical power acquired because of varying wet snow and dry snow rates is depicted in Fig. 11 & 12. The received optical power for different snow rate is different, but the received optical power for dry snow is less compared to wet snow. So, from this, it has been revealed that in dry snow fall condition, the Laser beam attenuated more compared to wet snow.

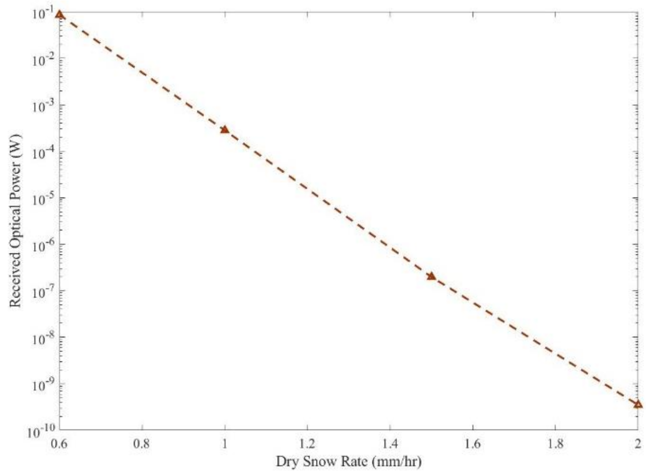

Fig. 11 Received optical power Vs different wet snow rates

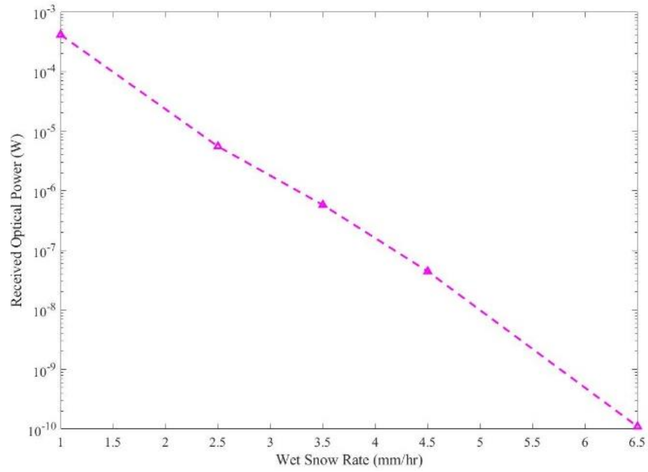

Fig. 12 Received optical power Vs different dry snow rates

4.2. Pointing Loss at the Receiver and Transmitter Sides

Since the appropriate line of sight phenomena between the transmitter and receiver sides is essential to the operation of the FSO system, pointing loss is another crucial component. A significant degree of pointing error may have happened during the formation of the optical link between the transmitter and receiver if the correct line of sight is not maintained. The pointing error angle of the transmitter and receiver sides, as well as the transmitter gain ($G_{Transmitter}$) and receiver gain ($G_{Receiver}$), all affect the pointing loss of the transmitter and receiver sides. The gain of the transmitter side and the receiver side, respectively, might be expressed using equations (18), and (19) [54].

$$G_{Transmitter} = \frac{\pi D_T}{\lambda} \tag{18}$$

$$G_{Receiver} = \frac{\pi D_R}{\lambda} \tag{19}$$

After employing a beam expander, the wavelength (λ) and diameter (D_T) of the optical source determine the transmitter gain, and the wavelength and receiver diameter ($D_{Receiver}$) determine the receiver gain as well. Finally, equations (20) and (21) respectively represent the pointing loss factor of the transmitter side and receiver side.

$$l_{pT} = \exp(-G_{Transmitter} * \theta_T^2) \tag{20}$$

$$I_{pR} = \exp(-G_{Receiver} * \theta_R^2) \tag{21}$$

θ_T and θ_R are the corresponding pointing error angles for the transmitter and receiver sides.

As can be seen from Fig 13, the allowable pointing error angle is smaller at the lower visibility range than it is at the higher visibility circumstances because optical power loss is often larger at lower visibility conditions than it is at higher visibility conditions. The higher wavelength (1550 nm) optical Laser source offers a more allowable pointing error angle than other IR & visible wavelengths from a lower visibility range in higher visibility weather situations, which is another point that has been illustrated from the same picture.

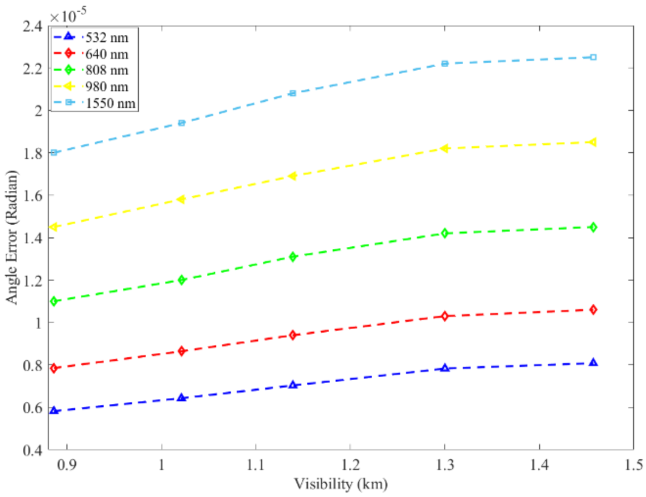

Fig. 13 Pointing error angle at various levels of visibility

The pointing error angle for the transmitter and receiver side at various rain rates is shown in Fig. 14. In order to preserve the intended BER value (10^{-6}), the pointing error angle is also altered from a high value to a low value since the optical power loss is low to high for the low to high rate of rain.

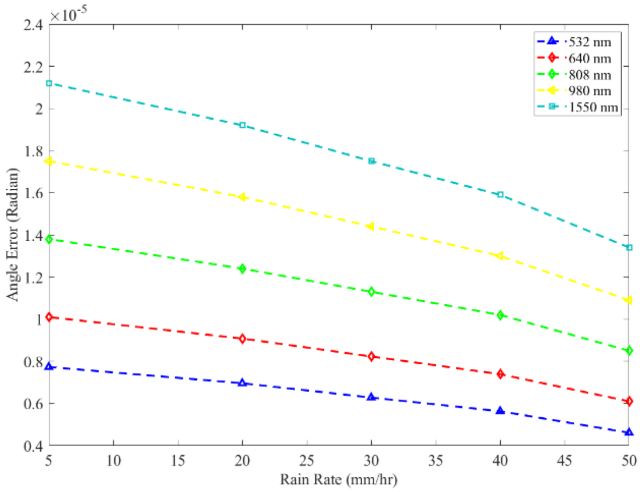

Fig. 14 Pointing error angle at various levels of Rain Rates

The pointing error angle for the transmitter and receiver side of varying wet snow rate, and dry snow rate is shown in Fig. 15 and 16 respectively.

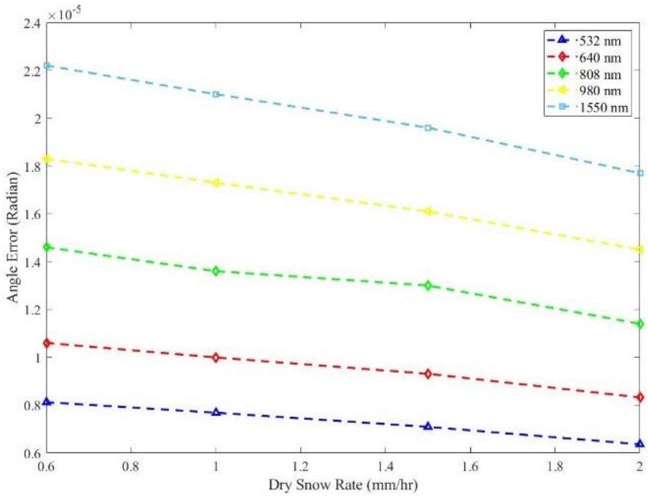

Fig. 15 Pointing error angle at various levels of Dry snow rate

The pointing error angle is also altered from a high value to a low value in order to maintain the required BER value (10^{-6}), since the optical power loss is low to high for the low to high rate of snow (dry and wet).

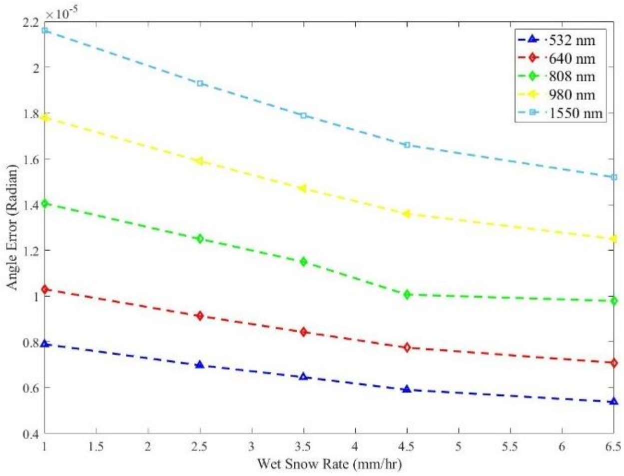

Fig. 16 Pointing error angle at various levels of Wet snow rate

4.3. Signal to Noise Ratio (SNR)

In photo-detector, SNR is the ratio of the generated signal current to the generated noise signal. The amount of generated signal current (I_P) in the photodetector depends upon the responsivity of the photo-detector (R_λ) and the incident optical signal on the photo-detector. The generated signal current is represented by equation (22).

$$I_P = P_R * R_\lambda \tag{22}$$

I_P indicates generated signal current, P_R represents received optical power on the photo-detector, R_λ indicates responsivity of photo-detector (A/W)

Thermal noise is occurred due to the thermal fluctuation of the electron in a photodetector or receiver circuit. The thermal noise variance is given in equation (23)[55][56]

$$\sigma_T = \sqrt{4 * k_B * Temp * \frac{BW}{R_L}} \tag{23}$$

Where, σ_T indicates thermal noise, k_B represents Boltzmann's constant, Temp indicates ambient temperature (300K considered), BW represents Bandwidth of photo-detector, R_L indicates Load resistance.

Dark current noise represents in equation (24)[55][56]

$$\sigma_D = \sqrt{2 * e * BW * I_d} \tag{24}$$

Where, σ_D represents dark current noise, e indicates Charge of electron, i_d indicates dark current of photo-detector

The Shot noise depends upon the background noise, the responsivity of the photo-detector, and generated signal current in the photo-detector, again background noise depends on the spectral radiance of the sky. The power of the receiver due to background noise (P_S) is given in equation (25)[57]

$$P_S = N_B * \tau_r * B_{OF} * (\pi * \frac{D_R}{2} * \frac{FOV}{2})^2 \tag{25}$$

Where N_B indicates Irradiance (W/m^{2}µm) τ_r represents receiver optics transmittance, B_{OF} indicates bandwidth of optical filter, D_R represents Receiver (photo-detector) aperture, FOV indicates field of view of receiving lens.

Therefore, the shot noise current represents in equation (26),

$$i_s = I_P + (P_S * R_\lambda) \tag{26}$$

I_s indicates total shot current, P_S represents the power of the receiver due to background noise.

The shot noise can be represented by equation (27)[56][57]

$$\sigma_S = \sqrt{2 * e * BW * i_S} \tag{27}$$

Where, σ_S indicates Shot current noise, i_s denotes Shot current of photo-detector

The total signal to noise (dB) ratio is determined by the equation (28)[56][57]

$$SNR = 10 * \log(\frac{I_p}{\sqrt{\sigma_T^2 + \sigma_S^2 + \sigma_D^2}}) \tag{28}$$

In essence, SNR has been reliant on the intensity of the optical signal at the receiving end of a specific connection distance. However, increasing the rate of rain or snow has significantly reduced or weakened the optical signal intensity. Equations 10 and 14 have already been used to illustrate the attenuation of optical power caused by rain and snow. Once more, equation 17 has demonstrated that the optical power received at the receiver side directly affects the produced current signal at the receiver side. According to equation 28, the SNR value is likewise directly related to the amount of current produced at the receiver or photodetector. As a result, the SNR value is dominantly dependent upon the rain rate as well as snow rates.

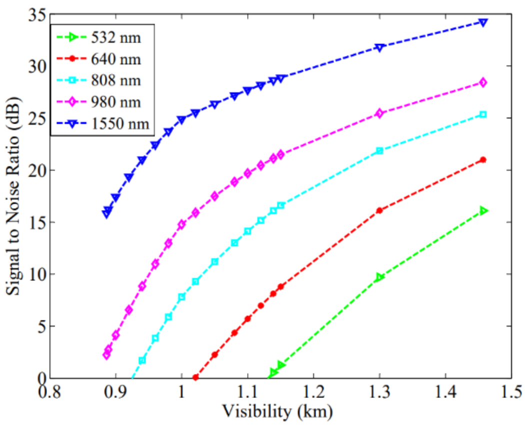

Fig. 17 Signal to Noise ratio Vs Visibility

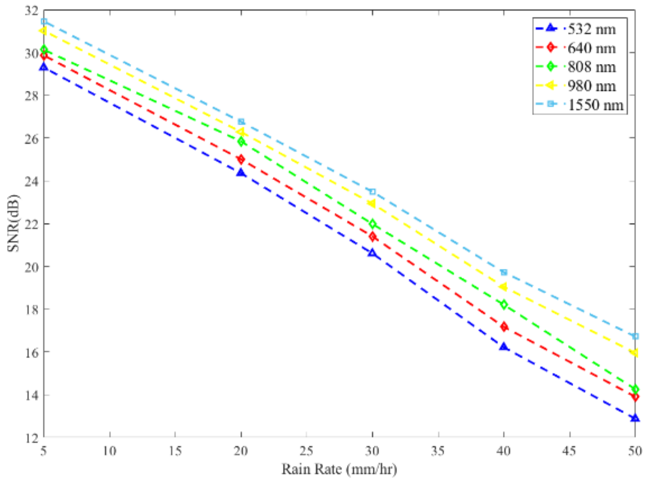

Fig. 18 Signal to Noise ratio Vs different levels of rain rates

In order to retain the same efficiency, the responsivity varies for each wavelength under consideration from the receiver's perspective.

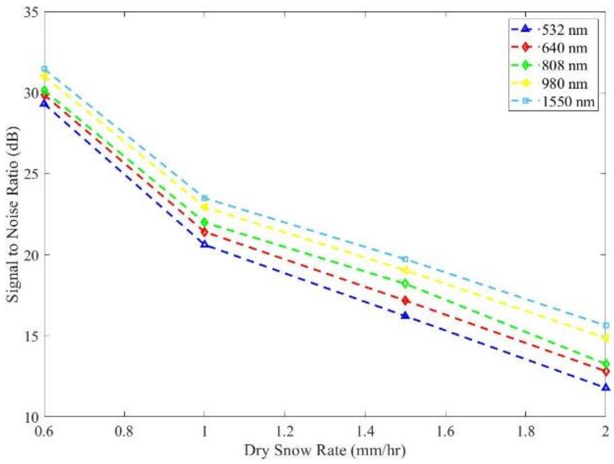

Fig. 19 Signal to Noise ratio Vs different levels of dry snow rates

As a result, the shot noise varies depending on the wavelength. Corresponding to this, the solar background noise varies with wavelength due to variations in the sun irradiance ($W.m^{-2}.nm^{-1}$) factor. Because of this, the signal-to-noise ratio varies depending on the wavelength, and the BER varies depending on the wavelength due to the SNR's variable value. Fig 16 shows the various SNR values resulting from the various visibility ranges in the foggy situations. The scattering coefficient is lower at 1550 nm than other wavelengths since fog occurrences are often wavelength-dependent, with the exception of situations in which the vision range is shorter than 500 m (as per the KIM model).

Rain and snow conditions are wavelength independent phenomena, meaning that the received optical power is nearly constant over a range of rain and snow rates. However, because the produced signal current in the photodetector varies, the SNR and BER values have varied for the various wavelengths. To keep the photodetector system's optical efficiency, the wavelengths' responsiveness varies. Another reason for variations in SNR and related BER values is that the noise figure varies between wavelengths.

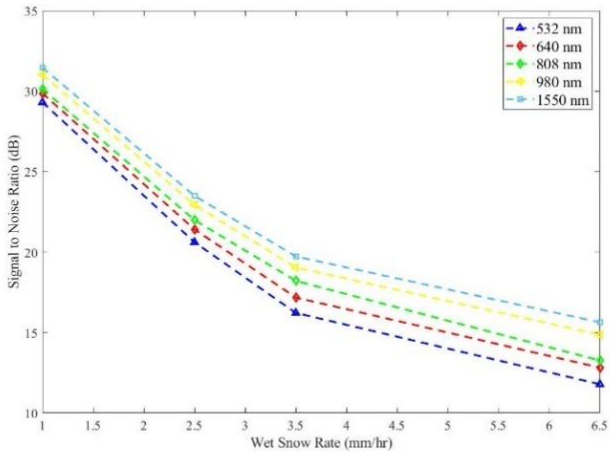

Fig. 20 Signal to Noise ratio Vs different levels of wet snow rates

The SNR fluctuates with varying rain rates, respectively, as seen in Fig. 18. Fig. 19 shows the various SNR values for various dry snow rates, whereas Fig. 20 shows the comparable SNR values for various wet snow rates. The data makes it evident that the SWIR wavelength (1550 nm) outperform the visible & other IR wavelengths.

4.4. Bit Error Rate (BER)

The reliability of the terrestrial-based FSO system can be expressed by the probability of bit error which is called Bit Error Rate (BER). Smaller the Bit Error Rate, the more reliable the FSO communication system. The value of BER is dependent upon directly the received signal level and photo-detector noise level.

Moreover, the RZ-OOK modulation scheme is considered, the BER of the above mention modulation scheme is given by equation (29) [58][59]. The Signal to Noise ratio and corresponding Bit Error Rate of different wavelength Laser sources and different visibility (up to 1.5 km.) is illustrated in Fig 21.

$$BER_{RZ-OOK} = \frac{1}{2} * erfc(\frac{\sqrt{SNR}}{2}) \tag{29}$$

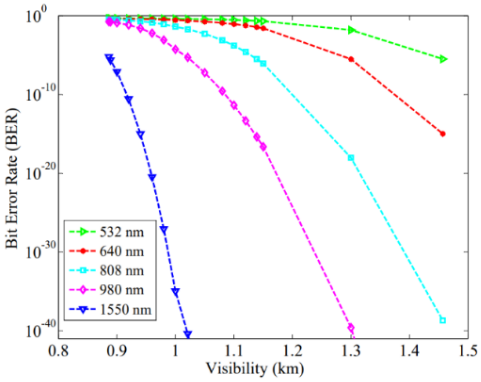

Fig. 21 Bit Error Rate Vs Visibility

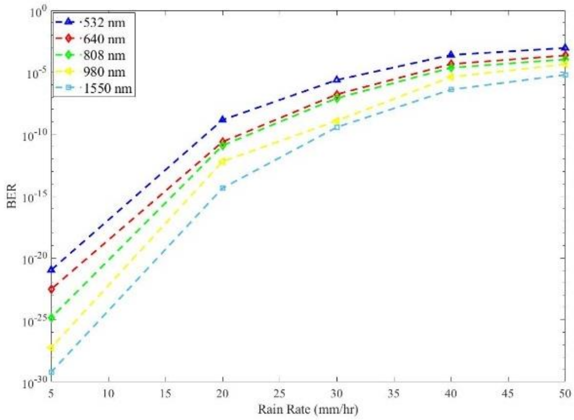

Fig. 22 Bit Error Rate Vs different level of rain rates

As the SNR varies, the BER also changes in different atmospheric conditions like rain, & snowy (wet & dry) conditions.

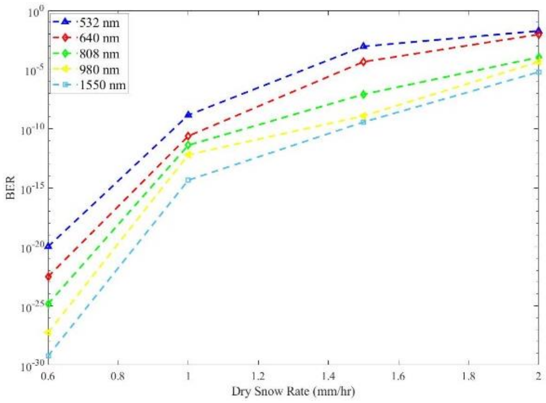

Fig. 23 Bit Error Rate Vs different level of dry snow rates

Fig. 22, Fig. 23 & Fig. 24 show the BER variation due to different level of rain rates, snow rates (dry & wet).

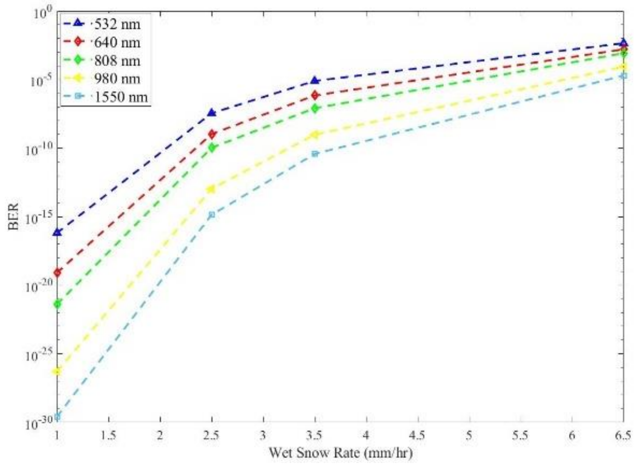

Fig. 24 Bit Error Rate Vs different level of wet snow rates

In all the aforesaid considered atmospheric anomalies conditions, with an increment of anomalies rate the performance of BER is increased, irrespective of wavelengths.

5. Link Margin for Different Wavelength Coherent Optical Sources

The link margin for above mentioned different wavelength Laser source using terrestrial-based FSO calculation is shown in Table 6, the link range considered is 5 km at a data rate of 100 MHz using a photo-detector of 125 MHz bandwidth.

Table 8 Link margin of different wavelength Laser sources at a link range of 5 km

	Different Wavelength				
Parameter	532 nm	640 nm	808 nm	980 nm	1550 nm
Transmitted peak Laser output power	+30 dBm	+30 dBm	+30 dBm	+30 dBm	+30 dBm
Transmitter optical loss	-0.2 dB	-0.2 dB	-0.2 dB	-0.2 dB	-0.2 dB
Atmospheric loss for clear sky condition (Visibility > 30 km.)	-1.8 dB	-1.4 dB	-1.05 dB	-0.82 dB	-0.45 dB
Scintillation Loss ($C_n^2 = 10^{-16} m^{-2/3}$)	-3.2 dB	-2.8 dB	-2.5 dB	-2.2 dB	-1.7 dB
Receiver optical loss (Consider Convex lens & Optical Filter)	-1.55 dB	-1.55 dB	-1.55 dB	-1.55 dB	-1.55 dB
Photo-detector sensitivity for 16 dB SNR	-32 dBm	-33 dBm	-34.2 dBm	-35.4 dBm	-37 dBm
Obtained link margin	~ 56 dB	~ 57 dB	~ 59 dB	~ 60.6 dB	~ 63.1 dB

Mainly, two reasons are responsible for the variation of the link margin of different Laser sources are used in terrestrial FSO link. The first reason is the optical power attenuation of different wavelength in different atmospheric conditions are not same. As seen from the 'Beer Lambert' law, the lower range of optical wavelength is more attenuated than the higher range of optical wavelength, when it is propagated through the atmospheric channel. Therefore, received optical power at the receiver side is not the same for all considered wavelengths. Another reason is the generated signal current in the photodetector which is dependent upon the received optical power and responsivity of the photo-detector. As the responsivity of the photo-detector of each wavelength is different so the generated signal current is different for different wavelengths which creates an impact on photo-detector sensitivity. Shot noise or background noise which is generated in photo-detector, dependent on the spectral irradiance of sky, this value is (the value of irradiance is different with different values of wavelength, in general, the values of irradiance for 532 nm, 640 nm, 808 nm, 980 nm, and 1550 nm are 1200 W/m^{2}µm, 1160 W/m^{2}µm, 910 W/m^{2}µm, 605 W/m^{2}µm, 210 W/m^{2}µm) [60] different for different wavelength. This can create an impact on photo-detector sensitivity for different wavelength Laser sources. As a result, the link margin value is varying for different wavelength optical sources and SWIR wavelengths are given the higher link margin value. The terrestrial link using aforesaid wavelengths can be worked in atmospheric visibility condition is summarized in Table 7. This table depicts the maximum permissible limit of visibility of fog using 5 km link range and different wavelengths are considered.

Table 9 Link margin matrix for 5 km link range with different Laser sources in foggy weather conditions

Wavelengths				
532 nm	640 nm	808 nm	980 nm	1550 nm
Visibility: 1.45 km	Visibility: 1.3 km	Visibility: 1.14 km	Visibility: 1.02 km	Visibility: 0.88 km
Rain Rate: 33.0 mm/hr	Rain Rate: 33.9 mm/hr	Rain Rate: 34.8 mm/hr	Rain Rate: 35.6 mm/hr	Rain Rate: 36.4 mm/hr
Dry Snow Rate: 1.4 mm/hr	Dry Snow Rate: 1.5 mm/hr	Dry Snow Rate: 1.62 mm/hr	Dry Snow Rate: 1.75 mm/hr	Dry Snow Rate: 1.94 mm/hr
Wet Snow Rate: 4.2 mm/hr	Wet Snow Rate: 4.8 mm/hr	Wet Snow Rate: 5.6 mm/hr	Wet Snow Rate: 6 mm/hr	Wet Snow Rate: 6.5 mm/hr

As the link margin is different for different considered wavelengths, therefore, the link performance has been different for different considered wavelength for a particular environmental situation. From the Table 8, it has been depicted that 1550 nm Laser source provides highest link margin & 532 nm provides lower link margin, as a result 1550 nm provides better link performance in lower visibility as well as higher visibility condition, whereas 532 nm performs worse in lower as well as higher visibility condition.

From the link margin table, it can be seen that the 1550 nm Laser source offers a link margin of 63.1 dB followed by the 980 nm Laser source which offers a link margin of 60.6 dB. Hence, from the cost-effective or economic point of view, 980 nm Laser source may be used in terrestrial FSO system instead of 1550 nm Laser source. In case of visible light communication systems, 640 nm Laser source may give an effective result than 532 nm Laser source.

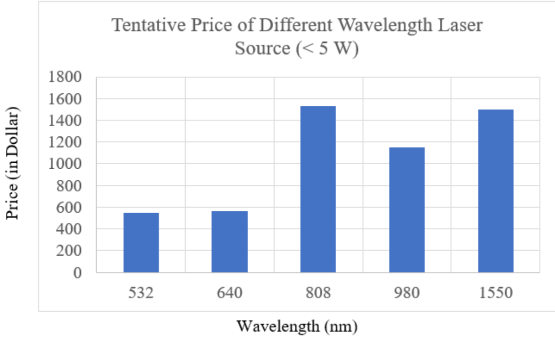

Fig. 25 Tentative price of considered different wavelength Laser Source [61][62]

Fig. 25 presents a preliminary cost estimate for the various wavelengths of laser sources under consideration. This cost study has demonstrated that the cost of the 980 nm laser is less than that of the 1550 nm laser source. InGaAs-type photodetectors are typically needed for 1550 nm wavelength laser sources because they have greater response at this wavelength than Si type detectors, which are not appropriate for this wavelength. Conversely, 980 nm wavelength responds in Si and InGaAs types of photodetectors. However, this study has taken into consideration an InGaAs type detector for a 980 nm laser source. When considering cost-effectiveness, Si detectors are more economical than InGaAs type detectors. Fig. 26 shows the tentative price of of p-i-n type Si & InGaAs photodetector.

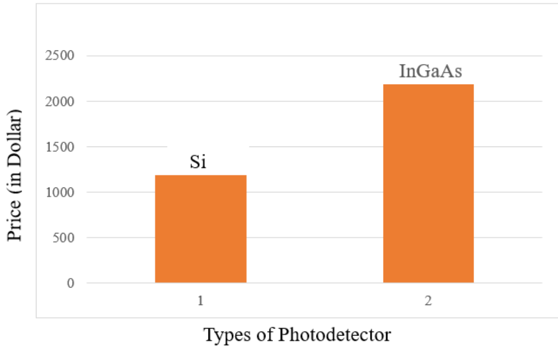

Fig. 26 Tentative price of p-i-n type Si & InGaAs photodetector [63][64][65]

6. Conclusion

In this article, a detailed comparative study of different wavelengths like 532 nm, 640 nm, 808 nm, 980 nm, 1550 nm in different atmospheric conditions, has been analyzed with corresponding actual technical specifications of optical accessories. These accessories are required in a typical terrestrial FSO communication system. Therefore, from this study, it has been found that the SWIR wavelength Laser source (1550 nm) poses as a better option in the foggy weather situations than other wavelengths especially, the visible Laser sources.

The attractive features of a typical FSO system make it suitable for remote applications. This system can also be used to establish different networks like building to building, ground to hill, hill to hill, military application, tactical communication, etc. In disaster areas, where a temporary link is required due to the disintegration of any existing communication link, this system can perform very well. The main drawback of the terrestrial FSO system is that the optical beam or optical power is attenuated by atmospheric anomalies like rain, fog, etc. The primary disadvantage of this kind of system is its extreme reliance on the weather. Under very unfavorable weather circumstances, this device can malfunction or stop working altogether. Consequently, efforts are being made in a number of countries to improve system resilience during inclement weather. Various diversity methods, such as Multiple Input Single Output (MISO), Single Input Multiple Output (SIMO), and Multiple Output Multiple Input (MIMO) etc., are well-known for their ability to reduce the atmospheric attenuation level [66][67][68][69]. In the event of unfavorable weather, the wavelength diversity scheme (using mid-wave infrared) may be advantageous [70][71][72][73][74][75]. A further noteworthy deployment is the integration of this system with the traditional radio frequency system [76]. In inclement weather, the RF system is turned on and the FSO is turned off. To install this type of terrestrial FSO system as per requirement, in the above-mentioned applications area, this comparative study can be resourceful. Compared to other wavelengths, the 1550 nm laser source works better in various atmospheric anomalies and offers a superior pointing error angle in both favourable and unfavourable weather situations. The technical specifications of optical accessories mentioned in this article may help to estimate the link performance for a longer link range (5 km), subjected to hazardous atmospheric conditions for establishing reliable communication.

The five principal wavelengths, which are phenomena, have been linked to the current investigation. Longer connection distance was also linked to this study. The main atmospheric factors are taken into account, and using carefully selected optics, the impact of each meteorological factor on each wavelength is thoroughly assessed. Consequently, the link margin has been successfully raised. Finally, the link margin has been assessed for each wavelength after accounting for the pointing error in this simulation.

This system is mostly used in disaster situations when traditional internet connections have failed or been damaged. In these cases, it may be quickly set up for short-term communication needs. The results of this study's evaluation of several wavelengths, including visible, SWIR, and others, show the link margins for each wavelength separately. Several relevant investigations have been conducted from the literature survey portion (in the introduction section), although the link distance has not been very great, and comparisons have been made at a maximum of two or three wavelengths for a certain atmospheric condition. Prior to deploying this kind of system in specific application areas, however, a thorough investigation with suitable optical accessories has been conducted with five significant wavelengths and various significant atmospheric scenarios. This study was conducted with a large link distance (5 km). By suitably choosing the optical accessories, the link margin has been increased efficiently.

REFERENCES

[1] A. Malik and P. Singh, "Free Space Optics: Current Applications and Future Challenges", *Int. J. Optics*, vol. 6, pp. 1-7, 2015.

[2] Z. Ghassemlooy, W. O. Popoola and S. Rajbhandari, *Optical Wireless Communications System and Channel Modelling with MATLAB*, chapter 2, CRC press, 2012.

[3] B. Bhattacharjee, P. K. Sadhu, A. Ganguly and A. K. Naskar, "Integrated Green Submersible Pumping System for Future Generation", *FU Elec. Energ.*, vol. 34, no. 1, pp. 37-51, 2021.

[4] B. Bhattacharjee, A. Chakrabarti and P. K. Sadhu., "Solar Photovoltaic Integrated Pump for Advanced Irrigation System", *Int. J. Innov. Technol. Explor. Eng.*, vol. 8, no. 8, pp. 3246-3250, 2019.

[5] S. M. A. Shah, M. S. A. Latiff and R. Tahir, "Performance Measurement of Free-Space Optical 980 nm Channel Using Multiple Sets of Environmental Conditions", *Wirel. Pers. Commun.*, vol. 85, pp. 345-357, 2015.

[6] T. Manna, A. Das, B. Bhattacharjee and S. Mukherjee, "Robust Communication Strategy for Overcoming Narrowband Jamming in Low-Frequency CDMA-DSSS System Using MATLAB", *FU Elec. Energ.*, vol. 37, no. 3, pp. 531-540, 2024.

[7] S. Ghoname, H. A. Fayed, A. A. El Aziz and M. H. Aly, "Performance Analysis of FSO Communication System: Effects of Fog, Rain and Humidity", In Proceedings of the Sixth International Conference on Digital Information Processing and Communications (ICDIPC), 2016, pp. 151-155.

[8] M. M. Shumani, M. F. L. Abdullah and A. Z. Suriza, "The Effect of Haze Attenuation on Free Space Optics Communication (FSO) at Two Wavelengths under Malaysia Weather", In Proceedings of the International Conference on Computer and Communication Engineering (ICCCE), 2016, pp. 459-464.

[9] Shaina, A. Gupta, "Comparative Analysis of Free Space Optical Communication System for Various Optical Transmission Windows under Adverse Weather Conditions", In Proceedings of the Twelfth International Multi-Conference on Information Processing, 2016.

[10] A. Tripathi, G. G. Soni, S. Gupta and S. A. Mandloi, "Experimental Investigation of Wind and Temperature Induced Scintillation Effect on Optical Wireless Communication Link", *Optik*, vol. 178, pp. 1248-1254, 2019.

[11] G. G. Soni, A. Tripathi, M. Shroti and K. Agarwal, "Experimental Study of Rain Affected Optical Wireless Link to Investigate Regression Parameters for Tropical Indian Monsoon", *Opt. Quantum Electron.*, vol. 55, p. 384, 2023.

[12] G. G. Soni, A. Tripathi, A. Mandloi and S. Gupta, "Compensating rain induced impairments in terrestrial FSO links using aperture averaging and receiver diversity", *Opt. Quantum Electron.*, vol. 51, p. 244, 2019.

[13] A. Tripathi, S. Gupta and A. Mandloi, "Investigation of Weather Effects Toward Convergence of Wired and Wireless Gigabit Services Over Hybrid Free-Space Optical Link", *Opt. Eng.*, vol. 60, no. 2, p. 026102, 2021.

[14] G. G. Soni, A. Tripathi, A. Mandloi and S. Gupta, "Effect of Wind Pressure and Modulation Schemes on Rain Interrupted Optical Wireless Links Under Tropical Climates", *Opt. Quantum Electron.*, vol. 51, p. 172, 2019.

[15] S. Chaudhary, X. Tang, Z. Ghassemlooy, B. Lin, X. Wei and S. K. Liaw, "A 3 × 25 Mbps WDM-Ro-VLC System for Amateur Radio Applications", In Proceedings of the 2nd West Asian Colloquium on Optical Wireless Communications (WACOWC), 2019, pp. 6-10.

[16] S. K. Modalavalasa, R. Miglani, S. Chaudhary, F. Tubbal and R. Raad, "Developing Cost-Effective and High-Speed 40 Gbps FSO Systems Incorporating Wavelength and Spatial Diversity Techniques", *Front. Phys.*, vol. 9, p. 744160, 2021.

[17] Anuranjana, S. Kaur, R. Goyal and S. Chaudhary, "1000 Gbps MDM-WDM FSO Link Employing DP-QPSK Modulation Scheme Under the Effect of Fog", *Optik*, vol. 257, p. 168809, 2022.

[18] P. Liang, C. Zhang, J. Nebhen, S. Chaudhary and X. Tang, "Cost-Efficient Hybrid WDM-MDM-Ro-FSO System for Broadband Services in Hospitals", *Front. Phys.*, vol. 9, p. 732236, 2021.

[19] C. Zhang, P. Liang, J. Nebhen, S. Chaudhary, A. Sharma, J. Malhotra and B. Sharma, "Performance Analysis of Mode Division Multiplexing-Based Free Space Optical Systems for Healthcare Infrastructure's", *Opt. Quantum Electron.*, vol. 53, p. 635, 2021.

[20] S. Chaudhary, L. Wuttisittikulkij, J. Nebhen, X. Tang, M. Saadi, S. A. Otaibi, A. Althobaiti, A. Sharma and S. Choudhary, "Hybrid MDM-PDM Based Ro-FSO System for Broadband Services by Incorporating Donut Modes Under Diverse Weather Conditions", *Front. Phys.*, vol. 9, p. 756232, 2021.

[21] N. Xiaolong, Y. Haifeng, L. Zhi, C. Chunyi, M. Ce and Z. Jiaxu, "Experimental Study of the Atmospheric Turbulence Influence on FSO Communication System", In Proceedings of Asia Communications and Photonics Conference, 2018, pp. 1-3.

[22] M. A. Esmail, H. Fathallah and M. S. Alouini, "An Experimental Study of FSO Link Performance in Desert Environment", *IEEE Commun. Lett.*, vol. 20, no. 9, pp. 1888-1891, 2016.
[23] A. Khandakar, A. Touati, F. Touati, A. Abdaoui and A. Bouallegue, "Experimental Setup to Validate the Effects of Major Environmental Parameters on the Performance of FSO Communication Link in Qatar", *Appl. Sci.*, vol. 8, no. 12, p. 2599, 2018.
[24] S. Malik and P. K. Sahu, "A Study on Free Space Optical Communication for Bhubaneswar City", In Proceedings of USNC-URSI Radio Science Meeting, 2017, pp. 101-102.
[25] S. M. Yasir, N. Abas and M. S. Saleem, "Performance Analysis of 10Gbps FSO Communication Link Under Suspended Dust and Rain Conditions in Lahore, Pakistan", *Nonlinear Opt. Quantum Opt.*, vol. 0, pp. 1-18, 2019.
[26] R. Nebuloni and C. Capsoni, "Laser Attenuation by Falling Snow", In Proceedings of the 6th International Symposium on Communication Systems, Networks and Digital Signal Processing, 2008, pp. 265-269.
[27] A. Kesarwani, Anuranjana, S. Kaur, M. Kaur and P. S. Vohra, "Performance Analysis of FSO Link under Diferent Conditions of Fog in Delhi, India", In Proceedings of the 2nd IEEE International Conference on Power Electronics, Intelligent Control and Energy Systems (ICPEICES), 2018, pp. 958-961.
[28] M. A. Esmail, H. Fathallah and M. S. Alouini, "Outdoor FSO Communications Under Fog: Attenuation Modeling and Performance Evaluation", *IEEE Photonics J.*, vol. 8, no. 4, pp. 1-22, Aug. 2016.
[29] https://www.ulooptics.com/beam-expanders/
[30] H. Kaushal, G. Kaddoum, V. K. Jain and S. Kar, "Experimental Investigation of Optimum Beam Size for FSO Uplink", *Opt. Commun.*, vol. 400, pp.106-114, 2017.
[31] S. Mukherjee, S. Paul and S. Mazumdar, "A Cost Effective FSO Communication Link Using 808 nm Laser and its Performance Analysis in Simulated Temperature Conditions", *Opt. Quantum Electron.*, vol. 55, pp. 1-15, 2023.
[32] B. Das, S. Mukherjee, B. Chattopadhyay and S. Mazumdar, "Design of a 10 GHz Optical Wireless Communication Link Using Low Power C-band Laser Diode", *Result in Opt.*, vol. 5, pp. 1-11, 2021.
[33] A. G. Alkholidi and K. S. Altowij, "Free Space Optical Communications -Theory and Practices" in *Wireless Communications*, 2014.
[34] S. Mukherjee, S. Paul and S. Mazumdar, "Effect of MIMO Scheme on MWIR FSO Link & Comparison with SWIR Wavelength in the Presence of Different Visibility and Strong Turbulence Circumstances", *J. Opt. Commun.*, vol. 45, no. s1, pp. s1977-s1983, 2023.
[35] S. K. Mandal, B. Bera and G. G. Dutta, "Free Space Optical(FSO) Communication Link Design Under Adverse Weather Condition", In Proceedings of International Conference on Computer, Electrical & Communication Engineering (ICCECE), 2020, pp. 1-6.
[36] Thorlabs, InGaAs Amplified Photodetectors, Fixed Gain. [Online] Available at: https://www.thorlabs.com/newgrouppage9.cfm?objectgroup_id=4#1897
[37] A. B. Stephen, *Optical Communication Receiver Design*, SPIE Optical Engineering Press, 1997.
[38] H. Kaushal, V. K. Jain and S. Kar, *Free Space Optical Communication*, Springer India, 1st Ed, 2017.
[39] S. Mukherjee, S. Paul and S. Mazumdar, "Experimental Studies of FSO Communication Channel Using Visible Wavelengths Coherent Optical Sources in Artificial Rainy Condition", In Proceedings of 2022 IEEE Calcutta Conference (CALCON), Kolkata, India, 2022, pp. 98-103.
[40] Z. Ghassemlooy and W. O. Popoola, "Terrestrial Free-Space Optical Communication" in *Mobile and Wireless Communications Network and Circuit Level Design*, chapter 17, Intech, 2010.
[41] M. C. Baddock, C. L. Strong, J. F. Leys, S. K. Heidenreich, E. K. Tews and G. H. McTainsh, "A Visibility and Total Suspended Dust Relationship", *Atmos. Environ.*, vol. 89, pp. 329-336, 2014.
[42] T. S. Sarkar, B. Sinha, S. Mukherjee, I. Jaradar and S. Mazumdar, "Development of an FPGA Based Indoor FSO Communication System Using 808 nm Infrared Laser Source", In Proceedings of 2020 IEEE Calcutta Conference (CALCON), Kolkata, India, 2020, pp. 313-317.
[43] I. I. Kim, B. McArthur and E. J. Korevaar, "Comparison of Laser Beam Propagation at 785 nm and 1550 nm in Fog and Haze for Optical Wireless Communications", Proceedings of SPIE-The International Society Optical Engineering, vol. 4214, pp. 1-12, 2001.
[44] S. Mukherjee, B. Das and S. Mazumdar, "Experimental Studies of Laser Power Attenuation of 532 nm Laser at Different Visibility Using Simulated Foggy Conditions", *AIP Conf. Proc.*, vol. 2640, p. 020029 2022.
[45] M. Twati, M. Badi and F Adam, "Analysis of Rain Effects on Free Space Optics Based on Data Measured in the Libyan Climate", *Int. J. Inform. Electron. Eng.*, vol. 4, no. 6, pp. 469-472, 2014.
[46] S. Chaudhary and A. Amphawan, "The Role and Challenges of Free-space Optical Systems", *J. Opt. Commun.*, vol. 35, no. 4, pp. 327-334, 2014.

[47] S. Mukherjee, S. Paul and S. Mazumdar, "Experimental Studies and Analysis of 1550 nm Laser as Optical Wireless Communication Link in Simulated Rainy, Foggy and Heating Conditions According to Indian Atmosphere", *Light Eng.*, vol. 31, pp. 19-33, 2023.

[48] P. W. Kruse, L. D. McGlauchlin and R. B. McQuistan, *Elements of Infrared Technology: Generation, Transmission, and Detection*, J. Wiley & Sons, New York, 1962.

[49] L. C. Andrews, R. Phillips and C. Y. Hopen, *Laser Beam Scintillation with Applications*, Bellingham, WA, USA: SPIE; 2001.

[50] E. Jackman and P. Pusey, "Significance of K-distributions in Scattering Experiments", *Phys. Rev. Lett.*, vol. 40, no. 9, p. 546, 1978.

[51] M. Al-Habash, L. C. Andrews and R. L. Phillips, "Mathematical Model for the Irradiance Probably Density Functions of a Laser Beam Propagating Through Turbulent Media", *Opt. Eng.*, vol. 40, no. 8, p. 200410, 2001.

[52] S. Parween and A. Tripathy, "Free Space Optic Communication Using Optical AM, OOK-NRZ and OOK-RZ Modulation Techniques", In Proceedings of the 3rd International Conference on Electronics, Materials Engineering & Nano-Technology (IEMENTech), 2019, pp. 1-4.

[53] N. A. Mohammed, A. El-Wakeel and M. H. Aly "Pointing Error in FSO Link under Different Weather Conditions", *Int. J. Video Image Process. Netw. Secur.*, vol. 12, no. 1, pp. 6-9, 2012.

[54] S. Singh and G. Soni, "Pointing Error Evaluation in FSO link", In Proceedings of the Fifth International Conference on Advances in Recent Technologies in Communication and Computing (ARTCom), 2013, pp. 365-370.

[55] M. K. El-Nayal, M. M. Aly, H. A. Fayed and R. A. AbdelRassoul, "Adaptive Free Space Optic System Based on Visibility Detector to Overcome Atmospheric Attenuation", *Results in Phys.*, vol. 14, p. 102392, 2019.

[56] H. J. Kbashi, M. A. Hameed and S. A. Shykre, "Calculations of Signal to Noise Ratio (SNR) for Free Space Optical Communication Systems", *Um-Salama Sci. J.*, vol. 5, no.1, pp. 95-100, 2008.

[57] R. Barrios and F. Dios, "Wireless Optical Communications Through the Turbulent Atmosphere: A Review" in *Optical Communications System*, Chapter 1, Intech, 2011.

[58] M. A. A. Ali, "Comparison of NRZ, RZ-OOK Modulation Formats for FSO Communications under Fog Weather Condition", *Int. J. Comput. Appl.*, vol. 108, no. 2, pp. 29-34, 2014.

[59] S. Mukherjee, S. Paul and S. Mazumdar, "Experimental Studies of the Influence of Scintillation on a FSO Communication System for Visible and Infrared Wavelengths", *J. Russian Laser Res.*, vol. 44, pp. 357-364, 2023.

[60] V. Vaida, J. S. Daniel, H. G. Kjaergaard, L. M. Goss and A. F. Tuck, "Atmospheric Absorption of Near Infrared and Visible Solar Radiation by the Hydrogen Bonded Water Dimmer", *Q. J. R. Meteorol. Soc.*, vol. 127, pp.1627-1643, 2001.

[61] Laser Diode Source, "How much does a laser diode cost?". [Online] Available at: https://www.laserdiodesource.com/how-much-does-a-laser-diode-cost

[62] Roithner LaserTechnik Price list. [Online] Available at: https://www.roithner-laser.com/pricelist.pdf

[63] Hamamatsu InGaAs PIN photodiode, Part Number: G12180-110A specifications. [Online] Available at: https://www.indiamart.com/proddetail/ingaas-pin-photodiode-23949488712.html

[64] Hamamatsu Si Pin Photodiode, Part Number: S5821-03 specifications. [Online] Available at: https://www.indiamart.com/proddetail/si-pin photodiode23931285830.html?srsltid=AfmBOorrANF8K_FHNcdJkJYSX0HGafiPyPtqxWSNzsXFF3 Z6bapOfhf4

[65] Thorlabs, Free-Space Balanced Amplified Photodetectors [Online] Available at: https://www.thorlabs.com/ newgrouppage9.cfm?objectgroup_id=1299

[66] P. Kaur, V. K. Jain and S. Kar, "Performance Analysis of FSO Array Receivers in Presence of Atmospheric Turbulence", *IEEE Photonics Technol. Lett.*, vol. 26, pp. 1165-1168, 2014.

[67] P. Kaur, V. K. Jain and S. Kar, "Performance Analysis of Free Space Optical Links Using Multi-Input Multi-Output and Aperture Averaging in Presence of Turbulence and Various Weather Conditions", *IET Commun.*, vol. 9, no. 8, pp.1104-1109, 2015.

[68] P. Kaur, V. K. Jain and S. Kar, "BER Performance Improvement of FSO Links with Aperture Averaging and Receiver Diversity Technique Under Various Atmospheric Conditions", In Proceedings of the 9th International Conference on Industrial and Information Systems (ICIIS), 2014, pp. 1-6.

[69] B. Das, S. Mukherjee, B. Chattopadhyay and S. Mazumdar, "Design of a 10 GHz Optical Wireless Communication Link Using Low Power C-band Laser Diode", *Results in Opt.*, vol. 5, p. 100129, 2021.

[70] J. Mikolajczyk, R. Weih and M. Motyka, "Optical Wireless Link Operated at the Wavelength of 4.0 μm with Commercially Available Interband Cascade Laser", Sensors, vol. 21, no. 12, p. 4102, 2021.

[71] T. Liu, J. Zhang, C. Zhu, Y. Lei, C. Sun and R. Zhang, "Investigation of the Wavelength Selection for the Free Space Optical Communication System", In Proceedings of the Asia Communications and Photonics Conference (ACP), 2018, pp. 1-3.

[72] S. M. Johnson, E. Dial and M. Razeghi, "High-speed Optical Communications Based Quantum Cascade Lasers and Type-II Superlattice Detectors", In Proceedings of SPIE OPTO, 2020, p. 1128814.

[73] J. L. Miller, *Principles of Infrared Technology: A practical guide to the State of the Art*, New York: Springer, 1994.

[74] Q. Hao, G. Zhu, S. Yang, K. Yang, T. Duan, X. Xie, K. Huang and H. Zeng, "Mid-Infrared Transmitter and Receiver Modules for Free-Space Optical Communication", *Appl. Opt.*, vol. 56, no. 8, pp. 2260-2264, 2017.

[75] J. Mikolajczyk and D. Szabra, "Integrated IR modulator with a Quantum Cascade Laser", *Appl. Sci.*, vol. 11, no. 14, p. 6457, 2021.

[76] M. A. A. Ali, S. A. Adnan and S. A. Al-Saeedi, "Transporting 8×10 Gbps WDM Ro-FSO Under Various Weather Conditions", *J. Opt. Commun.*, vol. 41, no. 1, pp. 99-105, 2020.